Article

Disks of Oxygen Vacancies on the Surface of TiO$_2$ Nanoparticles

Vladimir B. Vykhodets [1,*], Tatiana E. Kurennykh [1] and Evgenia V. Vykhodets [2]

1   Institute of Metal Physics UB RAS, 18 S.Kovalevskaya Street, 620108 Ekaterinburg, Russia
2   Ural Federal University, 19 Mira Street, 620002 Ekaterinburg, Russia
*   Correspondence: vykhod@imp.uran.ru

Abstract: Oxide nanopowders are widely used in engineering, and their properties are largely controlled by the defect structure of nanoparticles. Experimental data on the spatial distribution of defects in oxide nanoparticles are unavailable in the literature, and in the work presented, to gain such information, methods of nuclear reactions and deuterium probes were employed. The object of study was oxygen-deficient defects in TiO$_2$ nanoparticles. Nanopowders were synthesized by the sol–gel method and laser evaporation of ceramic targets. To modify the defect structure in nanoparticles, nanopowders were subjected to vacuum annealings. It was established that in TiO$_2$ nanoparticles there form two-dimensional defects consisting of six titanium atoms that occupy the nanoparticle surface and result in a remarkable deviation of the chemical composition from the stoichiometry. The presence of such defects was observed in two cases: in TiO$_2$ nanoparticles alloyed with cobalt, which were synthesized by the sol–gel method, and in nonalloyed TiO$_2$ nanoparticles synthesized by laser evaporation of ceramic target. The concentration of the defects under study can be varied in wide limits via vacuum annealings of nanopowders which can provide formation on the surface of oxide nanoparticles of a solid film of titanium atoms 1–2 monolayers in thickness.

Keywords: nanoparticles; TiO$_2$; oxygen vacancies; nuclear reactions; deuterium probes

1. Introduction

The physico-chemical and functional properties of oxide nanoparticles, which are widely employed in engineering, are largely dependent on the defect structure of nanoparticles, namely, the concentration of point defects, their type, and spatial distribution. In this field, works have mainly been devoted to defects that condition oxygen deficiency in nanoparticles compared to the stoichiometry [1,2]. In addition, oxygen vacancies and clusters based on them strongly affect the electrical, magnetic, diffusion, catalytic, and other properties of oxide nanopowders [3–5]. For example, a concept of d^0-magnetism was proposed [6], which helped to explain ferromagnetic properties observed on oxide nanopowders that did not contain any magnetic dopants by an oxygen deficiency in nanoparticles. Such results were obtained on the oxide powders of TiO$_2$, Al$_2$O$_3$, ZnO, In$_2$O$_3$, HfO$_2$, CuO, and others [7–11].

The majority of results concerning the defect structure of oxide nanoparticles are obtained for the TiO$_2$ nanoparticles with the use of a large number of techniques [3,5,8,12–15]. They highlight a wide variety of types of point defects and the evolution of the defect structure under different treatments of nanopowders, say, oxygen annealing [3]. When investigating the defect structure, the most informative were the methods of positron annihilation [3,5,8,12–15], X-ray photoelectron spectroscopy [3,5,13], and photoluminescence [14]; as defects, there were specified oxygen and titanium vacancies [3,8], interstitial titanium atoms [12], 3D vacancy clusters [8], complexes consisting of oxygen and titanium vacancies [3], Ti^{3+} ions and oxygen vacancies [15], and others [12]. The diversity of defect types in the oxide nanoparticles is conditioned by a large number of atoms on the sample surface, the presence of defects - charge carriers, mixed cation valence, changing oxygen concentration upon different powder treatments, etc.

With the bulk of important results accumulated on the types of defects in the oxide nanoparticles and their impact on the magnetic properties of nanoparticles [3,16–20], the state-of-art in this field can hardly be considered sufficient. First, no measurements of the oxygen concentration were performed and, hence, it was not accounted for in the concentration balance. For this reason, it cannot be excluded that information on several defect types is lacking. The more probable it seems to take into account the selective sensitivity of many techniques to defects of different types. Second, there are no available experimental data on the spatial distribution of defects in nanoparticles gained by direct observations. Such experiments are necessary since the energy states of atoms near the surface and in the bulk are drastically different.

In view of the above, this work is devoted to studying the defect structure of oxide nanoparticles via measurements of the oxygen concentration and using a technique that allows the determination of the defect concentration on the surface and in the bulk of nanoparticles. The choice of TiO_2 nanoparticles as the object for investigation is conditioned by a wide scope of practical applications of the dioxide titanium nanopowders [21–25]. The oxygen concentration was measured by the method of nuclear reactions (NRA); the error of measurements being about 0.5–1.0%, which makes it applicable only for nanopowders with rather a large oxygen deficiency compared to stoichiometry, at a level of several percent. Nanopowders of TiO_2 meet this condition [26]. The defect concentration was determined by the method of deuterium probes (DP) [2]. It is based on the dependence of the deuterium solubility in the oxide particles on the concentration of defects of a specified type. The application of the DP method was reasonable since, first, it is sensitive to defects bringing about oxygen deficiency [2] and, second, owing to a drastic difference in its basic principles from those of the earlier applied techniques, it enables one to detect defects of unknown types. The NRA and DP techniques have already been used to measure the oxygen and defect concentrations in oxide nanoparticles [2,26–28], but in these works, the type of defects and their spatial distribution in nanoparticles were not the subject of research.

2. Experimental

2.1. Synthesis of Oxide Nanopowders

Nanopowders were produced by the technology of laser evaporation of ceramic target (LE) [26] and sol–gel method (SG) [16,29]. As an LE, pills of titanium dioxide 60 mm in diameter were produced by pressing at room temperature, with the specific surface area of micropowder being 2 m^2/g. For vaporizing, a fiber-ytterbium laser was used with a wavelength of 1.07 µm and a maximal power output of 1 kW; the frequency of laser pulses was 5 kHz, duration was 50 µs. To produce nanopowders with a different specific area, the type of inert gas (argon or helium), gaseous pressure, and laser power were varied. For the synthesis of titanium oxide nanoparticles doped with cobalt ions by the SG method [29], acid hydrolysis of organometallic precursors was employed; in our case, titanium isopropyl oxide (Titanium (IV) isopropoxide) and cobalt (II) acetylacetonate as a source of metal ions. All reagents used were obtained from Sigma Aldrich. The preliminary required amounts of titanium isopropoxide (2 mL) and cobalt acetylacetonate complex were placed in a 5 mL test tube; then, 2 mL of acetone was poured into it. After vigorous shaking, a bluish-brown solution was formed. The solution was left overnight. Then, 1 mL of hydrochloric acid (0.1M) was poured into the solution. The hydrolysis reaction occurs almost instantly; however, for the process to run uniformly throughout the entire volume of the colloid, it was subjected to intensive ultrasonic action using an ultrasonic activator with a submerged titanium probe. Ultrasound exposure was 30 s. Then, the particles were separated by centrifugation (10,000 RPM) for 10 min and washed with acetone. The washing process was repeated three times. The resulting precipitate was dried at 70 °C. The precursor was further calcined in air at different temperatures (from 300 to 500 °C). Figure 1 shows micrographs of nanoparticles calcined at 400 and 500 °C, the image was obtained using transmission electron microscopy (TEM).
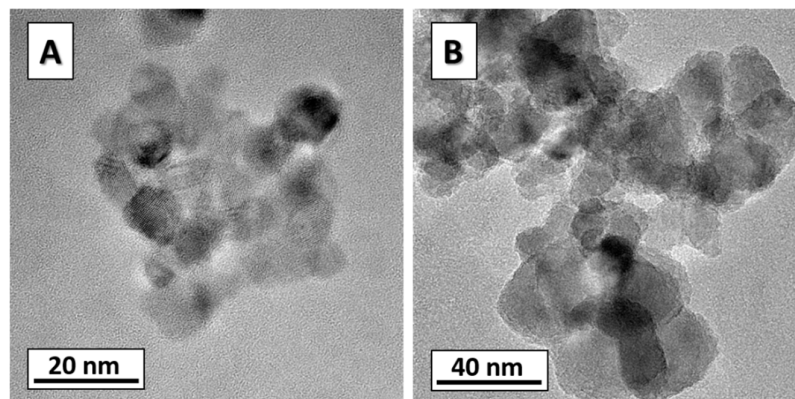
Figure 1. TEM micrographs of the TiO$_2$ nanoparticles calcined at 400 °C (**A**) and 500 °C (**B**).

2.2. Methods of Nuclear Reactions and Deuterium Probes

All nanopowders predominantly contained such phases of titanium dioxide as anatase, rutile, brookite, and their mixtures. Data on the phase composition are given in more detail in Section 3.1. In the current approach, the defect structure is characterized by the oxygen concentration C_O and defect concentration C_d and real defects contain a certain number of elementary point defects. Hence, a real defect can comprise vacancies and interstitial atoms of oxygen and titanium. Within the approach accepted, an oxygen vacancy cannot be distinguished from an interstitial titanium atom, the same as a titanium vacancy from an interstitial oxygen atom. When interpreting the results of studying the thus prepared samples, we considered solely oxygen vacancies as the most realistic elementary point defects. In the DP technique, after annealing in gaseous deuterium, nanopowders become three-component and their chemical composition can be presented by formula TiO$_{2-x}$D$_{2x/N}$, which accounts for the presence of 2 deuterium atoms per one defect [2]. Moreover, oxygen vacancies are supposed to be prone to joining in clusters, and N designates the amount of vacancies in a cluster. This formula enables easily obtaining that concentrations C_O and C_d are connected as follows

$$\frac{C_O}{C_O^0} = 1 - \frac{N+4}{3C_O^0}C_d,\qquad(1)$$

where C_O^0 is the oxygen concentration in a defectless oxide; herefrom, concentrations are expressed in fractions of the number of atoms in a nanoparticle. It is seen from Expression (1) that when treating the dependences $C_O(C_d)$, the number of vacancies in a defect N can be determined if oxygen vacancies are combined in complexes. Expression (1) is obtained for nanoparticles of arbitrary shape and does not depend on the spatial distribution of defects and mutual arrangement of vacancies in a cluster. For example, it is valid for cases when defects are distributed in a nanoparticle uniformly or only in its thin surface layer with vacancies forming in a cluster of both 2D and 3D complexes.

When using the method of LE, the average concentrations C_O and C_d were varied via the synthesis of nanopowders with different specific surface areas S. This approach makes it possible to produce nanopowders with different C_O and C_d, if the concentrations of defects in the bulk and near the surface are different. In the SG technology, nanopowders with different defect concentrations were produced using vacuum annealings. In the preliminary experiments, it was established that vacuum annealings are by no means a universal way of decreasing the oxygen concentration in the titanium dioxide nanopowders. In particular, in the case of undoped TiO$_2$, vacuum annealings exert a poor effect on the concentrations of oxygen and defects, which did not allow the analysis of the $C_O(C_d)$ dependence with reliable accuracy. At the same time, Co-doped nanopowders of TiO$_2$ with widely ranging oxygen concentrations were prepared using vacuum annealings. The same result was obtained in work [5], where it was shown that alloying of TiO$_2$ with cobalt

leads to increasing vacancy concentration. In view of this, in the case of the SG method, investigation of the dependence $C_O(C_d)$ was performed on powders alloyed with cobalt, its concentration in the cation sublattice made up of 3 at. %. Vacuum annealings were carried out after completion of the synthesis routine at temperatures varying from 200 to 500 °C and holding time, 15 to 30 min, 500 °C.

To measure the defect concentration using the DP method, first, nanopowders are annealed in gaseous deuterium, and then, the concentration of dissolved deuterium C_D is measured using the NRA technique. The DP method is shown in work [2] to be sensitive to defects bringing about oxygen deficiency in nanoparticles and is based on the existence of unambiguous relation of the C_d and C_D concentrations, which is provided by the formation of nanoparticles annealed in deuterium of clusters of a strictly specified composition. In particular, in the TiO_2 nanoparticles, one cluster consists of a defect and 2 deuterium atoms. The cluster composition was determined using the dependence of C_D on the dose of deuterium irradiation. In the current work, such a procedure was applied to all powders after synthesis and vacuum annealings, and the cluster composition was the same. In general, nanoparticles can contain defects of different types simultaneously. For example, in study [2], in the TiO_2 particles, along with defects detectable for the DP method, one more type of defect was observed, which consisted of Ti^{3+} ions and oxygen vacancies. The duration of deuterium annealing we used was, just as in [2], 1 h, with deuterium pressure being 0.6 atm. In the DP method, the determination of the defect concentration C_d is reduced to measuring the deuterium concentration C_D. For this reason, the metrological characteristics of the NRA technique for the reaction $^2H(d,p)^3H$ controlled the accuracy and sensitivity in the determination of the defect concentration C_d: statistical error made up several percent of the measured value and measurement sensitivity was about 0.01 at. %.

As was noted in Section 1, no experimental data on the spatial arrangement of defects in oxide nanoparticles are available in the literature. Such a task is objectively complicated because of the small size of nanoparticles. In the current work, a particular solution was obtained. It is based on an approach that involves the characterization of the defect structure using only two defect concentrations, namely, at the surface of nanoparticle C_{ds} and average concentration in the nanoparticle bulk C_{dv}. For the powders synthesized using LE, we investigated the dependence of defect concentration on the specific surface area $C_d(S)$, which allowed us to obtain, in the model with two concentration values C_{ds} and C_{dv}, information on the spatial distribution of defects in nanoparticles. For example, the growth of C_d with increasing S means higher defect concentration near the surface then in the bulk and vice versa. If $C_{ds} = C_{dv}$, the defect concentration C_d evidently is independent of S. In this work, of special interest was the case when defects to which the DP method is sensitive are localized near the nanoparticle surface. In this case, the chemical composition of nanopowders can be expressed by the formula $(1 - \Delta\rho S)TiO_2(\Delta\rho S)\left[(TiO_{2-y})D_{2y/N}\right]$, and the following relationship works:

$$C_d = \frac{\Delta y \rho S}{N(3 - \Delta y \rho S)},\qquad(2)$$

where ρ is the oxide density, Δ is the thickness of the oxygen-deficient layer whose chemical composition is denoted as TiO_{2-y}. Expression (2) is valid for particles of arbitrary shape. Hence, with equal parameters N, Δ, and y, in the powders with different specific area S, the dependence $C_d(S)$ will be close to linear, with the extrapolated value $C_d(0) = 0$. Since the DP method provides a high accuracy in measuring the defect concentration, in some particular cases the study of $C_d(S)$ can give reliable information on the ratio of defect concentrations in the bulk and near the nanoparticle surface. Note that application of this approach is bound to solely the case when powders are synthesized by LE technology. It favors independence of the parameters, Δ, and y of S, which will be considered in Section 3.2.

The average concentrations of oxygen C_O and deuterium C_D in nanopowders were determined by the NRA technique at a 2 MB van de Graaf accelerator using reactions $^{16}O(d,p_1)^{17}O^*$ and $^2H(d,p)^3H$ with the deuteron energy of 900 and 650 keV, respectively. In the majority of experiments in the accelerator, the samples were at room temperature and nanoparticles of powders were pressed into an indium plate. When the concentration C_O was measured at the temperature of 400 °C, nanoparticles were pressed into copper powder. Using Rutherford backscattering spectroscopy, it was established that indium or copper atoms were absent in the zone under analysis. The sample surface was set perpendicular to the incident beam, nuclear reaction products were registered with the use of a silicon surface barrier detector. The angle of proton registration was 160°, and the diameter of the incident beam was 1 or 2 mm. The irradiation dose was measured on the samples using a secondary monitor, with the statistical error being 0.2 to 1.0%. When mathematically processing the data, spectra from the samples under study were compared with those from reference samples having constant-in-depth isotope concentrations. For ^{16}O, it was CuO, whereas for deuterium, $ZrCr_2D_{0.12}$. In more detail, the experimental setting and processing procedure are described in work [2].

When doing this, it was necessary to provide highly accurate measurements of concentrations C_O and C_D, which was not trivial as the data on C_O depended on the presence on the nanoparticle surface of water molecules. With increasing the thickness of the water layer, the oxygen concentration in factions of the number of atoms in a nanoparticle decreases since the H_2O molecule contains fewer oxygen atoms than TiO_2. In view of this, the powders were dried under vacuum pumping-off. To monitor the oxygen concentration C_O, sampling measurements of the powders were performed in the accelerator chamber at 400 °C, which allows the elimination of the adsorbed water molecules. The results of the concentration C_D and C_d, unlike C_O, were not changed when varying experimental conditions, temperature, pressure, and annealing time. In addition, these results did not depend on the conditions of storing the powders for a year and more, since the deuterium annealing provided the elimination of water molecules from the nanoparticle surface. Figure 2 shows the spectra of protons p for the nuclear reactions $^{16}O(d,p_1)^{17}O^*$ and $^2H(d,p)^3H$, which were used to determine the oxygen and defect concentrations. The C_O and C_d concentrations are directly proportional to the number of registered protons, the shape of the spectra does not depend on C_O and C_d.
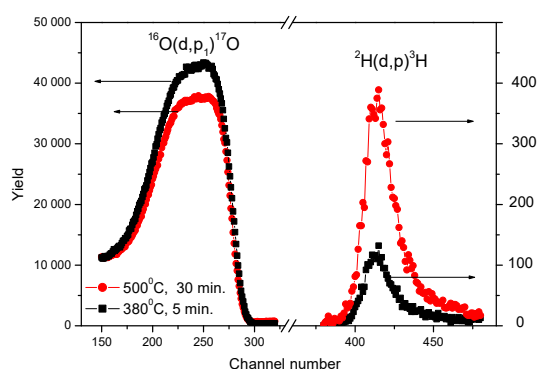

Figure 2. The spectra of products of the nuclear reactions $^{16}O(d,p_1)^{17}O^*$ and $^2H(d,p)^3H$ for the nanopowders synthesized by sol–gel method and annealed in vacuum. The temperatures and annealing times are shown in the figure.

3. Results and Discussion

3.1. Number of Oxygen Vacancies in a Defect

The dependence $C_O(C_d)$ shown in Figure 3 agrees with Expression (1), which testifies to the formation in the TiO_2 nanoparticles of defects consisting of oxygen vacancies. Processing by the least-square method gave the number of vacancies in a defect $N = 12.5 \pm 0.9$.
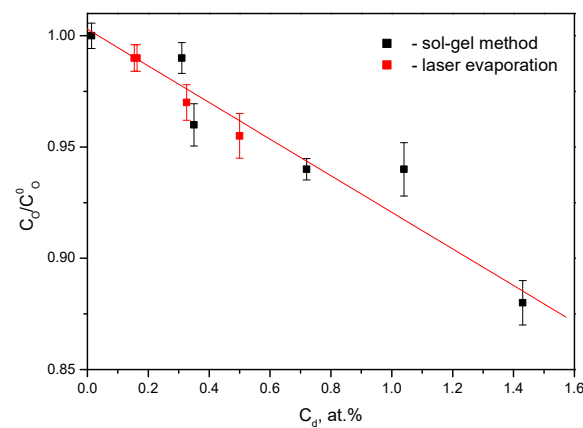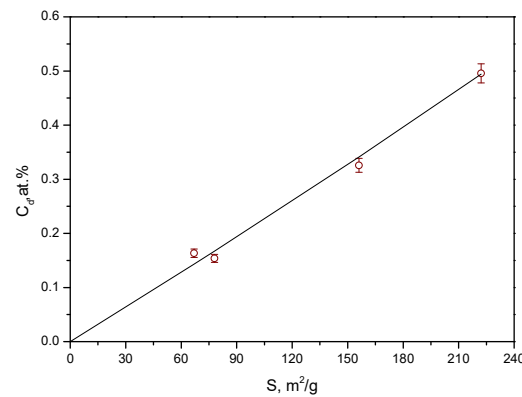
Figure 3. Dependence of the oxygen concentration C_O in TiO$_2$ nanopowders on the defect concentration C_d. Black points show results for powders synthesized by sol–gel method; red points, laser evaporation of ceramic target.

As follows from Figure 3, the formation in the dioxide titanium nanoparticles of defects containing $N = 12$ oxygen vacancies is invariant with respect to experimental conditions. First, it takes place in the nanopowders synthesized by different technologies and characterized by different mechanisms of defect formation. In the technology of SG method, in the as-synthesized powders of composition close to stoichiometric, the formation of defects occurs in the course of vacuum annealing through the oxygen depletion of nanoparticles. Upon LE, oxygen-deficient defects were formed directly in the course of synthesizing. Second, the powders strongly differ in the number of defects per unit volume of nanoparticles. This follows from Figure 2 since this parameter decreases with decreasing concentration C_O. Finally, the powders under study differed in phase composition. In the case of the SG method, it was anatase, whereas upon LE, the mixture of TiO$_2$ phases. In particular, in the powders with S > 200 m^2/g, brookite with small additions of anatase and rutile predominates, whereas at S < 200 m^2/g, quite the opposite, brookite was not observed at all, only anatase and rutile. Since the number of vacancies in a defect $N = 12$ does not depend on the synthesis technology, mechanism of defect formation, phase composition, and other characteristics of nanoparticles, one can suggest that the formation of such defects, denoted as Ti$_6$, is conditioned by thermodynamic reasons. This question needs further investigation.

3.2. Spatial Distribution of Defects Ti$_6$ in Nanoparticles

In the investigation of spatial distribution and size of defects consisting of 6 titanium atoms, different versions are considered, namely, defects located in the bulk and on the surface of nanoparticles and two-dimensional or three-dimensional ones. To obtain information on these issues, the dependence $C_d(S)$ was studied for the powders synthesized by the LE. As is seen in Figure 4, the experimental dependence $C_d(S)$ matches Expression (2) at constant parameters N, Δ, and y, which indicates that the defects consisting of 12 oxygen vacancies are located on the surface and absent in the bulk of TiO$_2$ nanoparticles.

Figure 4. Dependence of the defect concentration C_d on the specific surface area S of TiO$_2$ nanoparticles. Points are experimental data for the powders synthesized by laser evaporation of ceramic targets. Line is calculated by Expression (2) at $N = 12$ and $\Delta\rho$ y $= 7.56 \times 10^{-8}$ g/cm^2.

The independence of the parameter N on S was experimentally shown in Section 3.1. As for the parameters Δ and y, it is conditioned by the application of technology of LE. In this case, the formation of the defect structure of the surface layer proceeds in two steps. In the first step, at high temperatures in a vacuum, there form nanoparticles of stoichiometric composition in the bulk with the surface atomic layer virtually depleted of oxygen. It was established that the thickness of the oxygen-depleted layer does not depend on S and is equal to 0.36 nm [26], which approximately matches up an oxide monolayer. In works fulfilled within the theory of density functional, the following theoretical explanation of this result was given, namely, the existence of an oxygen-free layer on the oxide surface is energetically more favorable than of stoichiometric composition TiO$_2$ [26,30,31]. In the second step, the powder is cooled to room temperature in air and oxygen enters into the surface layer of nanoparticles. Evidently, in this case, the thickness of the oxygen-deficient layer does not depend on S. The amount of oxygen entering into nanoparticles depends on the regime of cooling the nanopowders. In this work, these regimes were the same for powders with different S.

We already mentioned above that the thickness of defects Ti$_6$ in nanoparticles synthesized by LE technology is within the atomic scale, whereas other linear dimensions are several times as high, i.e., the defects are two-dimensional. For nanoparticles synthesized by the SG method, no data on the spatial distributions of Ti$_6$ defects and inference on their two-dimensional or three-dimensional shape are presented in this work because of the lack of appropriate techniques. Yet, there are grounds to conclude that the Ti$_6$ defects in nanoparticles synthesized by the SG method also are two-dimensional and localized on the nanoparticle surface. In our opinion, these defects cannot occupy internal bulk regions of nanoparticles since the crystal structure of titanium dioxide with inner defects consisting of 12 oxygen vacancies will hardly be stable. At the same time, the presence of such defects on the surface of nanoparticles does not cause destruction of the crystal lattice of the oxide, which is evidenced by the results of works [26,30,31].

In the surface layer of TiO$_2$ particles, there are present two types of regions: (i) consisting of 6 titanium atoms and (ii) having composition close to stoichiometric TiO$_2$. It is worth estimating fractions of these regions. If to take up a constancy of distance between the titanium atoms upon the formation of the Ti$_6$ defect, the fraction of nanoparticle surface occupied by regions consisting of 6 titanium atoms is expressed as

$$\propto = \frac{1 - C_O/C_O^0}{\Delta\rho S(1 - C_O)} \leq 1. \tag{3}$$

In Figure 5, the dependences $\propto (C_O/C_O^0)$ calculated by Expression (3) for several values of S are shown. Points in Figure 5 show sampling experimental results, data on y

$\left(C_O/C_O^0\right)$ are also given. It is easy to show that the values of $\propto$ and y obey the expression $y = 2\propto$. Bends on the dependences $\propto \left(C_O/C_O^0\right)$ correspond to the formation on the nanoparticle surface of a solid monolayer in which oxygen atoms are absent. The horizontal portions of the dependences $\propto \left(C_O/C_O^0\right)$ correspond to the formation in nanoparticles of one more monolayer deficient in oxygen. It follows from Figure 5 that the fraction $\propto$ that is taken by regions consisting of 6 titanium atoms can be an easily controlled parameter. In particular, this refers to nanoparticles of TiO_2 produced by the SG method. In the as-synthesized state, they are virtually stoichiometric ($\propto \approx 0$), and by vacuum annealings and alloying with cobalt, this value can be increased to 1.
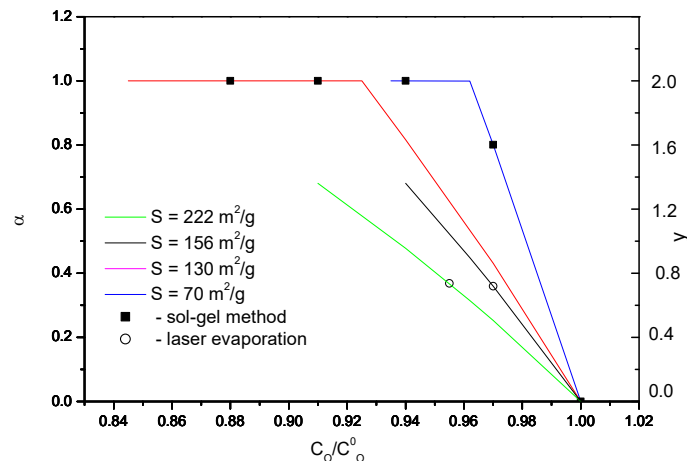
Figure 5. Dependence of the parameters $\propto$ and y for the surface monolayer of the titanium dioxide nanoparticles on the oxygen concentration C_O/C_O^0 in nanopowders. Lines show the calculation results by Expression (3): green—for nanopowders with the specific area 222 m^2/g; black, 156 m^2/g, red, 130 m^2/g, and blue, 70 m^2/g. Points are sampling results for the nanoparticles under study: filled ones refer to the powders synthesized by the sol–gel method; empty, laser evaporation of ceramic target.

It is shown that under certain conditions, in the TiO_2 nanoparticles there form two-dimensional defects consisting of 6 titanium atoms and localized on the nanoparticle surface, which results in a significant deviation of the chemical composition from the stoichiometry. Since, as noted in Section 1, in the TiO_2 nanoparticles there are present defects of other types, of interest is to compare the data on the concentration of surface two-dimensional defects with those obtained in previous studies. Unfortunately, in view of the absence of such information in works on oxide nanoparticles, we have to restrict ourselves to rough estimates. In a general case, defects of almost all types cause changes in the chemical composition of nanoparticles and their presence in the samples gives rise to a deviation from the linear dependence in Figure 3. Since in the work no deviations beyond the statistical experimental errors were registered, one can conclude that the concentration of other defects was far smaller than that of defects consisting of 6 titanium atoms.

4. Conclusions

Thus, new data on the defects that condition the oxygen deficit in the oxide nanoparticles of TiO_2 have been gained. The formed two-dimensional defects of atomic thickness are established to consist of six titanium atoms. They are free of oxygen atoms and located on the nanoparticle surface. The presence of such defects is detected in two cases: in the cobalt-doped nanoparticles of TiO_2 synthesized by the sol–gel method and subjected to vacuum annealings and undoped nanoparticles synthesized by laser evaporation of ceramic target. The data on the defect structure were obtained by the method of deuterium probes, DP, which was applied to measure the defect concentrations, and by nuclear reactions, NRA, to determine the oxygen concentration in nanopowders. The concentration of the

defects under study can be varied in wide limits; in particular, using vacuum annealings can provide gradual growth from 0 to 1.5 at. %, including the formation of a solid film of titanium atoms on the nanoparticle surface. The concentration of defects of other types in the nanoparticles under study was lower than that of two-dimensional defects located on the nanoparticle surface.

References

1.　Diebold, U. The surface science of titanium dioxide. *Surf. Sci. Rep.* **2003**, *48*, 53–229. [CrossRef]
2.　Vykhodets, V.B.; Kurennykh, T.E. Characterization of the defect structure of oxide nanoparticles with the use of deuterium probes. *RSC Adv.* **2020**, *10*, 3837–3843. [CrossRef] [PubMed]
3.　Ghosh, S.; Nambissan, P. Evidence of oxygen and Ti vacancy induced ferromagnetism in post-annealed undoped anatase TiO_2 nanocrystals: A spectroscopic analysis. *J. Solid State Chem.* **2019**, *275*, 174–180. [CrossRef]
4.　Mikhalev, K.N.; Germov, A.Y.; Ermakov, A.E.; Uimin, M.A.; Buzlukov, A.L.; Samatov, O.M. Crystal structure and magnetic properties of Al_2O_3 nanoparticles by ^{27}Al NMR data. *Phys. Solid State* **2017**, *59*, 514–519. [CrossRef]
5.　Qin, X.B.; Zhang, P.; Liang, L.H.; Zhao, B.Z.; Yu, R.S.; Wang, B.Y.; Wu, W.M. Vacancy identification in Co+doped rutile TiO_2 crystal with positron annihilation spectroscopy. *J. Physics: Conf. Ser.* **2011**, *262*, 012051. [CrossRef]
6.　Bouzerar, G.; Ziman, T. Model for Vacancy-Induced*d0d0*Ferromagnetism in Oxide Compounds. *Phys. Rev. Lett.* **2006**, *96*, 207602–207605. [CrossRef]
7.　Sundaresan, A.; Bhargavi, R.; Rangarajan, N.; Siddesh, U.; Rao, C.N.R. Ferromagnetism as a universal feature of nanoparticles of the otherwise nonmagnetic oxides. *Phys. Rev. B* **2006**, *74*, 161306. [CrossRef]
8.　Grosh, S.; Khan, G.G.; Mandal, K.; Samanta, A.; Nambissan, M.G. Evolution of Vacancy-Type Defects, Phase Transition, and Intrinsic Ferromagnetism during Annealing of Nanocrystalline TiO_2 Studied by Positron Annihilation Spectroscopy. *J. Phys. Chem. C* **2013**, *117*, 8458–8467. [CrossRef]
9.　Sudakar, C.; Kharela, P.; Suryanarayanan, R.; Thakurc, J.S.; Naikd, V.M.; Naika, R.; Lawesa, G. Room temperature ferromagnetism in vacuum-annealed TiO_2 thin films. *J. Magn. Magn. Mater.* **2008**, *320*, L31–L36. [CrossRef]
10.　Hong, N.H.; Sakai, J.; Poirot, N.; Brizé, V. Room-temperature ferromagnetism observed in undoped semiconducting and insulating oxide thin films. *Phys. Rev. B* **2006**, *73*, 132404. [CrossRef]
11.　Coey, J.M.D. High-temperature ferromagnetism in dilute magnetic oxides. *J. Appl. Phys.* **2005**, *97*, 10D313. [CrossRef]
12.　Murakami, H.; Onizuka, N.; Sasaki, J.; Thonghai, N. Ultra-fine particles of amorphous TiO_2 studied by means of positron annihilation spectroscopy. *J. Mater. Sci.* **1998**, *33*, 5811–5814. [CrossRef]
13.　Gaberle, J.; Shluger, A. The role of surface reduction in the formation of Ti interstitials. *RSC Adv.* **2019**, *9*, 12182–12188. [CrossRef] [PubMed]
14.　Jiang, X.; Zhang, Y.; Jiang, J.; Rong, Y.; Wang, Y.; Wu, Y.; Pan, C. Characterization of Oxygen Vacancy Associates within Hydrogenated TiO_2: A Positron Annihilation Study. *J. Phys. Chem. C* **2012**, *116*, 22619–22624. [CrossRef]
15.　Xu, N.N.; Li, G.P.; Pan, X.D.; Wang, Y.B.; Chen, J.S.; Bao, L.M. Oxygen vacancy-induced room-temperature ferromagnetism in D—D neutron irradiated single-crystal TiO_2 (001) rutile. *Chin. Phys. B* **2014**, *23*, 106101. [CrossRef]
16.　Doeuff, S.; Henry, M.; Sanchez, C.; Livage, J. The gel route to Cr^{3+}-doped TiO_2, an ESR study. *J. Non-Cryst. Solids* **1987**, *89*, 84–97. [CrossRef]
17.　Coey, J.M.D.; Venkatesan, M.; Stamenov, P. Surface magnetism of strontium titanate. *J. Phys.: Condens. Matter.* **2016**, *28*, 485001. [CrossRef]
18.　Ermakov, A.E.; Uimin, M.A.; Korolev, A.V.; Volegov, A.S.; Byzov, I.V.; Shchegoleva, N.N.; Minin, A.S. Anomalous Magnetism of the Surface of TiO_2 Nanocrystalline Oxides. *Fizika Tverdogo Tela* **2017**, *59*, 458–473. [CrossRef]
19.　Ahmed, S.A. Annealing effects on structure and magnetic properties of Mn-doped TiO_2. *J. Magn. Magn. Mater.* **2016**, *402*, 178–183. [CrossRef]

20.   Sokovnin, S.Y.; Balezin, M.E. Production of nanopowders using nanosecond electron beam. *Ferroelectrics* **2012**, *436*, 108–111. [CrossRef]

21.   Kamat, P.V. TiO_2 Nanostructures: Recent Physical Chemistry Advances. *J. Phys. Chem. C* **2012**, *116*, 11849. [CrossRef]

22.   Akdogan, N.; Nefedov, A.; Zabel, H.; Westerholt, K.; Becker, H.-W.; Somsen, C.; Gök, S.; Bashir, A.; Khaibullin, R.; Tagirov, L. High-temperature ferromagnetism in Co-implanted TiO_2 rutile. *J. Phys. D Appl. Phys.* **2009**, *42*, 115005. [CrossRef]

23.   Chen, Z.; Zhao, Y.S.; Ma, J.; Liu, C.; Ma, Y. Detailed XPS analysis and anomalous variation of chemical state for Mn- and V-doped TiO_2 coated on magnetic particles. *Ceram. Int.* **2017**, *43*, 16763–16772. [CrossRef]

24.   Cuaila, J.L.S.; Alayo, W.; Avellaneda, C. Ferromagnetism in spin-coated cobalt-doped TiO_2 thin films and the role of crystalline phases. *J. Magn. Magn. Mater.* **2017**, *442*, 212. [CrossRef]

25.   Li, D.; Li, D.K.; Wu, H.Z.; Liang, F.; Xie, W.; Zou, C.W.; Chao, L.X. Defects related room temperature ferromagnetism in Cu-implanted ZnO nanorod arrays. *J. Alloy. Comp.* **2014**, *591*, 80–84. [CrossRef]

26.   Vykhodets, V.; Johnson, K.G.; Kurennykh, T.E.; Beketov, I.V.; Samatov, O.M.; Medvedev, A.I.; Jarvis, E.A.A. Direct Observation of Tunable Surface Structure and Reactivity in TiO_2 Nanopowders. *Surf. Sci.* **2017**, *665*, 10–19. [CrossRef]

27.   Vykhodets, V.B.; Jarvis, E.A.A.; Kurennykh, T.E.; Beketov, I.V.; Obukhov, S.I.; Samatov, O.M.; Medvedev, A.I.; Davletshin, A.E.; Whyte, T. Inhomogeneous depletion of oxygen ions in oxide nanoparticles. *Surf. Sci.* **2016**, *644*, 141–147. [CrossRef]

28.   Vykhodets, V.B.; Jarvis, E.A.A.; Kurennykh, T.E.; Davletshin, A.E.; Obukhov, S.I.; Beketov, I.V.; Samatov, O.M.; Medvedev, A.I. Extreme deviations from stoichiometry in alumina nanopowders. *Surf. Sci.* **2014**, *630*, 182–186. [CrossRef]

29.   Uymin, M.A.; Minin, A.S.; Yermakov, A.Y.; Korolyov, A.V.; Balezin, M.Y.; Sokovnin, S.Y.; Konev, A.S.; Konev, S.F.; Molochnikov, L.S.; Gaviko, V.S.; et al. Magnetic properties and structure of TiO_2 -Mn (0.73%) nanopowders: The effects of electron irradiation and vacuum annealing. *Lett. Mater.* **2019**, *9*, 91–96. [CrossRef]

30.   Jarvis, E.A.A.; Carter, E.A. Metallic Character of the Al_2O_3(0001)-($\sqrt{31} \times \sqrt{31}$)R $\pm$ 9° Surface Reconstruction. *J. Phys. Chem. B* **2001**, *105*, 4045–4052. [CrossRef]

31.   Jarvis, E.A.A.; Carter, E.A. A nanoscale mechanism of fatigue in ionic solids. *Nano Lett.* **2006**, *6*, 505–509. [CrossRef] [PubMed]